Extensive Development of Precursory Helical Pairs Prior to Formation of Stereocomplex Crystals in Racemic Polylactide Melt Mixture

ARTICLE *in* MACROMOLECULES · JANUARY 2012

Impact Factor: 5.8 · DOI: 10.1021/ma2026995

4 AUTHORS, INCLUDING:

Jrjeng Ruan
National Cheng Kung University
17 PUBLICATIONS **182** CITATIONS
SEE PROFILE

An-Chung Su
National Tsing Hua University
96 PUBLICATIONS **1,966** CITATIONS
SEE PROFILE

Macromolecules

Article

pubs.acs.org/Macromolecules

Extensive Development of Precursory Helical Pairs Prior to Formation of Stereocomplex Crystals in Racemic Polylactide Melt Mixture

Ching-Feng Yang,[†] Yi-Fang Huang,[†,‡] Jrjeng Ruan,*[,‡] and An-Chung Su*[,†]

[†]Department of Chemical Engineering, National Tsing Hua University, Hsinchu 300, Taiwan

[‡]Department of Materials Science and Engineering, National Cheng Kung University, Tainan 701, Taiwan

Supporting Information

ABSTRACT: Melt crystallization of racemic polylactide (equimolar PLLA/PDLA) blend upon slow cooling (1 °C/min from 270 °C) was studied via a combination of wide-angle X-ray scattering (WAXS), differential scanning calorimetry (DSC), and Fourier-transform infrared spectroscopy (FTIR). Results indicated extensive development of racemic ($3_2/3_1$) helical pairs below 220 °C, followed by emergence of a broad mesomorphic peak in the WAXS profile below 190 °C; the intensity of this mesophase peak started to decrease at 150 °C, with concomitant emergence of WAXS- or DSC-discernible formation of stereocomplex (β_c) crystals. Isothermal measurements at 200 vs 170 °C revealed the presence of low vs high populations of helical pairs; β_c crystals were observed to develop only at 170 °C but not at 200 °C, indicating the need for adequate population of racemic helical pairs for formation of their mesomorphic clusters in the melt matrix as precursors of β_c nuclei. The clear change in the melt structure *well before* the formation of incipient β_c crystals reflects strong driving force under large supercooling toward transformation, but the transformation process is kinetically suppressed: only after extensive development of racemic helices and emergence of mesomorphic clusters in the melt matrix may nucleation occur. These observations suggest that the nucleation process proceeds in elementary units of preformed helical pairs in the melt matrix, with an intermediate stage of clustered helical pairs before incipience of β_c crystals.

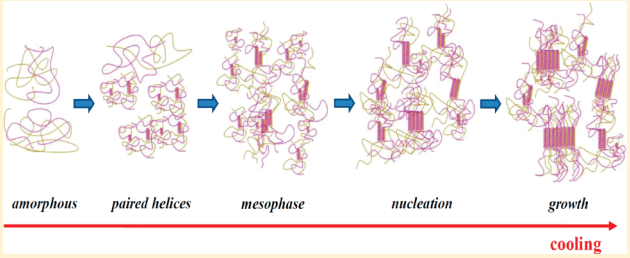

INTRODUCTION

Stereocomplexation is an interesting phenomenon observed in organic polymers. It has been reported to occur in blends of stereoisomeric polymers of different tacticity/chirality such as stereoisomers of poly(methyl methacrylate),[1,2] polythiirane,[3] polylactone,[4,5] polyoxirane,[6] and polylactide.[7] The common feature of the complex phase is that stereoisomeric chains are packed in pairs into a crystalline lattice of higher melting temperature (T_m) than that of the parent homopolymer crystals.

It was first reported[8] in 1987 that racemic stereocomplex of poly(L-lactide) (PLLA) and poly(D-lactide) (PDLA) may crystallize specifically into the β_c form with T_m strongly increased to ca. 210 °C as compared to the case of $T_m \approx 160$ °C for the α crystalline form of enantiomeric components. Okihara et al.[7] proposed that the β_c form is triclinic in structure (space group *P*1), with two chains per unit cell of parameters $a = b = 0.916$ nm, $c = 0.870$ nm, $\alpha = \beta = 109.2°$, and $\gamma = 109.8°$. On the basis of powder patterns from wide-angle X-ray scattering (WAXS) and results from molecular mechanics computations on the stereocomplex crystal, Brizzolara et al.[9] refined the triclinic unit cell parameters as $a = 0.912$ nm, $b = 0.913$ nm, $c = 0.930$ nm, $\alpha = \beta = 110°$, and $\gamma = 109°$. Cartier et al.[10] subsequently proposed a large trigonal cell that includes six chains per unit cell with $a = b = 1.498$ nm, $c = 0.870$ nm, $\alpha = \beta = 90°$, and $\gamma = 120°$ (space group *R*3*c*) in order to explain the triangular shape of single crystals of the PLLA/PDLA stereocomplex in terms of frustrated packing of paired 3_1-helical chains of opposite handedness. Ozaki et al.[11] and Sarasua et al.[12] studied the interaction of stereocomplex chains of polylactides during crystallization by means of Fourier-transform infrared spectroscopy (FTIR), revealing a shift of the C=O stretching band in β_c crystals to a lower wavenumber lower than the corresponding band in α crystals of the chiral counterpart. This band shift is accompanied by similar displacements in the C−H spectral bands. These results were interpreted in terms of specific C−H···O=C interactions between the paired stereoisomeric chains. More detailed assignments of conformation- or interaction-sensitive bands of polylactides were further made for both the chiral PLLA and the racemic PLLA/PDLA blend.[13−18]

Although structural features of the β_c crystalline form have been extensively studied and specific interactions for stereocomplexation between PLLA and PDLA have been addressed,

Received: December 14, 2011
Revised: January 2, 2012
Published: January 12, 2012

the process of the stereocomplex formation was not thoroughly examined. Whether PLLA/PDLA stereocomplexation occurs in solution or melt states *prior to* the formation of β_c crystals or during crystallization where PLLA (3_2) and PDLA (3_1) helices develop through crystallographic clipping (i.e., recognition/selection) and extension at the crystal growth front is still an open question. Here we report our recent observations on the ordering process of racemic PLLA/PDLA blend during melt crystallization upon slow cooling (1 °C/min) from deeply equilibrated melt state (270 °C) via time-resolved FTIR and WAXS, with supplementary differential scanning calorimetric (DSC) results. We show that only after extensive formation and subsequent clustering of paired helices may nucleation of β_c phase occur.

EXPERIMENTAL SECTION

Samples of PLLA and PDLA, both of weight-average molecular mass $M_w \approx 120$ kDa, were purchased from Sigma-Aldrich. Circular dichroism/polarimetry measurements indicated molar ellipticity $[\theta] = \pm 185°$ cm^2 g^{-1} at 228 nm and specific rotation $[\alpha]^{25} = \pm 155°$ at 633 nm. From the reported[19] value of $[\alpha]^{25} = 173°$ at 589 nm for PLLA of perfect optical purity, the chiral purity may be estimated as ca. 95% for both samples. Racemic PLLA/PDLA blend were prepared by admixing component polymers at 1:1 weight ratio into chloroform and vigorous stirring overnight, followed by quick evaporation of chloroform under reduced pressure and further vacuum-drying for 24 h to remove residual solvent.

FTIR spectra were recorded by use of a Perkin-Elmer Spectrum RXI Fourier-transform infrared spectrophotometer equipped with a Thermo Spectra Tech HT-32 high-temperature cell. Spectra were taken at a resolution of 2 cm^{-1} and averaged over 16 scans. Films on KBr pellets were cast from chloroform solutions containing 1 wt % racemic PLLA/PDLA blend and were vacuum-dried for 0.5 h. Film specimens were first heated to 270 °C for 15 min to erase previous thermal history and then cooled to room temperature at a rate of 1 °C/min, during which FTIR spectra were continuously monitored. In the case isothermal crystallization, the film specimens were first heated to 270 °C for 15 min, followed by cooling at a rate of 5 °C/min to and maintaining at 200 or 170 °C for time-resolved measurements.

WAXS studies of racemic blend films cast on glass substrates were made by use of an in-house Rigaku Ultima IV instrument equipped with a Cu Kα radiation source (with wavelength $\lambda = 1.542$ Å) operating at 40 kV and 20 mA and an INSTEC HCS302 high-temperature stage. DSC measurements for samples ca. 5 mg in weight were made by use of a Perkin-Elmer Diamond instrument routinely calibrated with high-purity indium and zinc standards and operated under a steady stream of protective nitrogen. In both WAXS and DSC studies, the same temperature programs as those in the FTIR studies were adopted for temperature- or time-resolved measurements.

RESULTS

Formation of Paired Helices in Melt. Given in Figure 1a–c are the temperature-resolved FTIR spectra of the racemic blend in respective ranges of 3100–2800, 1790–1720, and 1320–800 cm^{-1} upon cooling from 270 at 1 °C/min. It may be observed from Figure 1a that methyl C–H stretching (asymmetric vs symmetric, ca. 2990 vs 2940 cm^{-1}) and methine C$_\alpha$–H stretching band (2880 cm^{-1}) all shift slightly to lower frequencies with decreasing temperature; concomitantly, the intensity of the CH_3 asymmetry stretching band increased whereas intensities of CH_3 symmetric stretching/C$_\alpha$–H stretching bands decreased. These are more clearly demonstrated by corresponding difference spectra given in the Supporting Information as Figure S1. The broad C=O stretching band around 1750 cm^{-1} (cf. Figure 1b) suggests a distribution of local surroundings for carbonyl groups. With

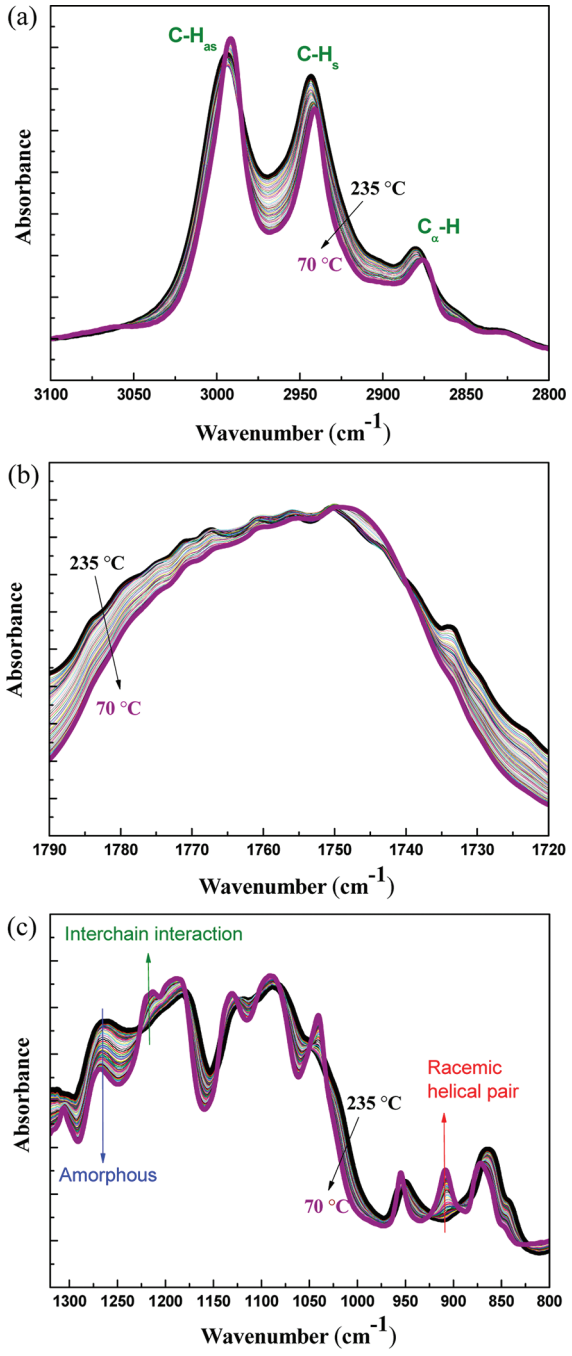

Figure 1. Temperature-resolved FTIR spectra in (a) the C–H stretching range of 3100–2800 cm^{-1}, (b) the C=O stretching range of 1790–1720 cm^{-1}, and (c) the fingerprint range of 1320–800 cm^{-1} collected during cooling of the racemic PLLA/PDLA blend at 1 °C/min from 270 °C. Note the decreased frequencies of the asymmetric vs symmetric C–H stretching peaks in (a), the general narrowing of the broad C=O stretching peak with delicate shifts of maximum position in (b), and the intensity changes of amorphous, interchain interaction, and $3_1/3_2$ helical peaks (around 1270, 1210, and 908 cm^{-1}, respectively) in (c).

decreasing temperature, there was a general narrowing of the C=O stretching band (signifying preference toward a specific molecular environment) with delicate shifts (as more clearly identifiable from the second-derivative curves in Figure S2) of maximum position toward lower wavenumbers. These observations suggest the development of weak interchain

dx.doi.org/10.1021/ma2026995 | *Macromolecules* 2012, 45, 872–878

CH···O=C hydrogen bonding.[11,12] Changes in peak positions of CH_3 asymmetry stretching and C=O stretching bands with temperature are given in Figure 2a, where significant changes in peak positions occur between 220 and 160 °C, beyond which the changes are more modest.

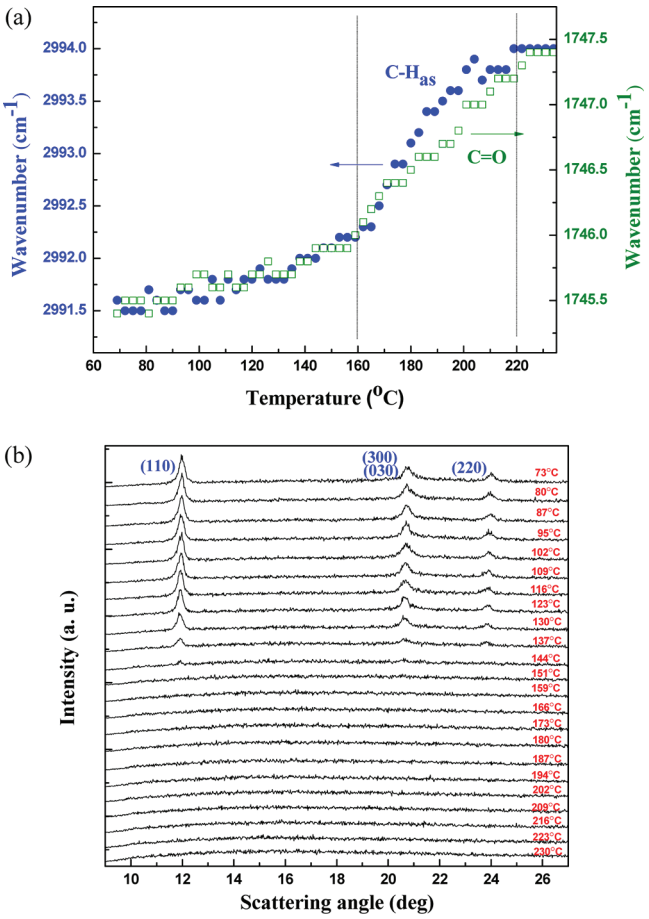

Figure 2. (a) Summary of variations of peak positions for C–H asymmetric stretching and C=O stretching bands in FTIR spectra shown in Figure 1a,b (as determined quantitatively from difference/derivative curves in Figure S1). (b) Corresponding WAXS profiles during cooling of the racemic blend at 1 °C/min from 270 °C.

Corresponding WAXS profiles shown in Figure 2b provide some clues to the molecular origins of spectral changes in Figure 1a,b. Upon cooling from 270 at 1 °C/min, the WAXS profiles remained featureless until reaching 150 °C where characteristic (110), (030)/(300), and (220) reflections of β_c crystals start to emerge at scattering angles $2\theta_B$ = 12.0°, 20.8°, and 24.1°, respectively. Intensities of these β_c reflections increased with further decreases in temperature below 150 °C. It hence appears that the development of interchain hydrogen bonding occurs well before crystallization.

This observation is further supported by intensity changes of the three key absorptions in the fingerprint region (cf. Figure 1c). The absorption at 908 cm^{-1}, assigned to the coupled C–C backbone stretching and CH_3 rocking mode, corresponds to racemic pair of $3_2/3_1$ helices; the absorption in the vicinity of 1210 cm^{-1} corresponds to coupled COC/CH_3 mode which is sensitive to interchain interactions, whereas the absorption around 1270 cm^{-1}, the coupled CH bending and COC stretching mode, is characteristic of the amorphous phase.[18]

Intensity changes of these three peaks with decreasing temperature are summarized in Figure 3. As may be observed

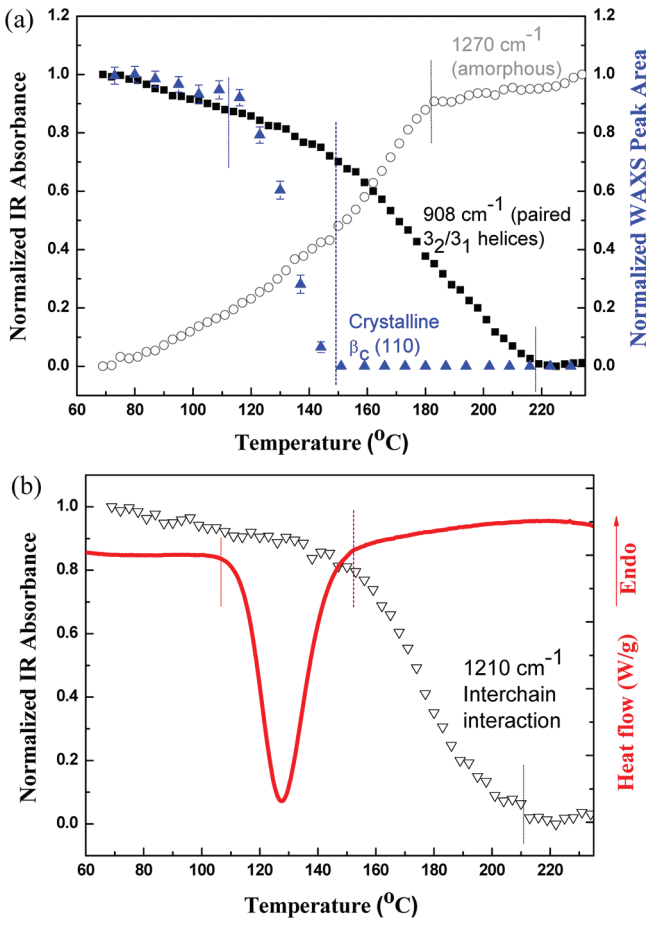

Figure 3. (a) Changes in normalized absorbance of helical peak at 908 cm^{-1} and amorphous peak at 1270 cm^{-1} (Figure 1c) and the WAXS (110) reflection of β_c crystals (Figure 2b) for racemic PLLA/PDLA blend during cooling (1 °C/min) from 270 °C. (b) Concomitant changes in normalized absorbance of interchain interaction peak at 1210 cm^{-1} (Figure 1c) and the parallel DSC cooling trace (also at 1 °C/min).

in Figure 3a, the 908 cm^{-1} band for paired helices was absent above 220 °C; the peak intensity rose quickly in the temperature range of 220 to 150 °C, beyond which the rate of increase slowed down significantly. This confirms unequivocally the extensive formation of coupled helices in the temperature range of 220 to 150 °C, well ahead of the emergence of β_c crystals below 150 °C as demonstrated by changes of the WAXS (110) reflection peak area (Figure 3a) and the parallel DSC cooling trace (Figure 3b). Also consistent with this picture is the gradual rise of the 1210 cm^{-1} absorption (characteristic of interchain interaction) between 220 and 150 °C (Figure 3b).

Clusters of Helical Pairs as Mesomorphic Precursors of β_c Nuclei. It is then intriguing to note from Figure 3a that the temperature-resolved intensity of the amorphous band around 1270 cm^{-1} exhibited a clear break at ca. 180 °C, with a lag of 40 °C behind the formation of paired helices at 220 °C yet ca. 30 °C ahead of the start of crystallization. This implies the existence of an intermediate state between the amorphous

dx.doi.org/10.1021/ma2026995 | *Macromolecules* 2012, 45, 872–878

phase (with or without isolated helical pairs) and the WAXS- or DSC-discernible β_c crystals.

As shown in Figure 4a, carefully deconvoluted WAXS profiles provide direct evidence for the existence of such a

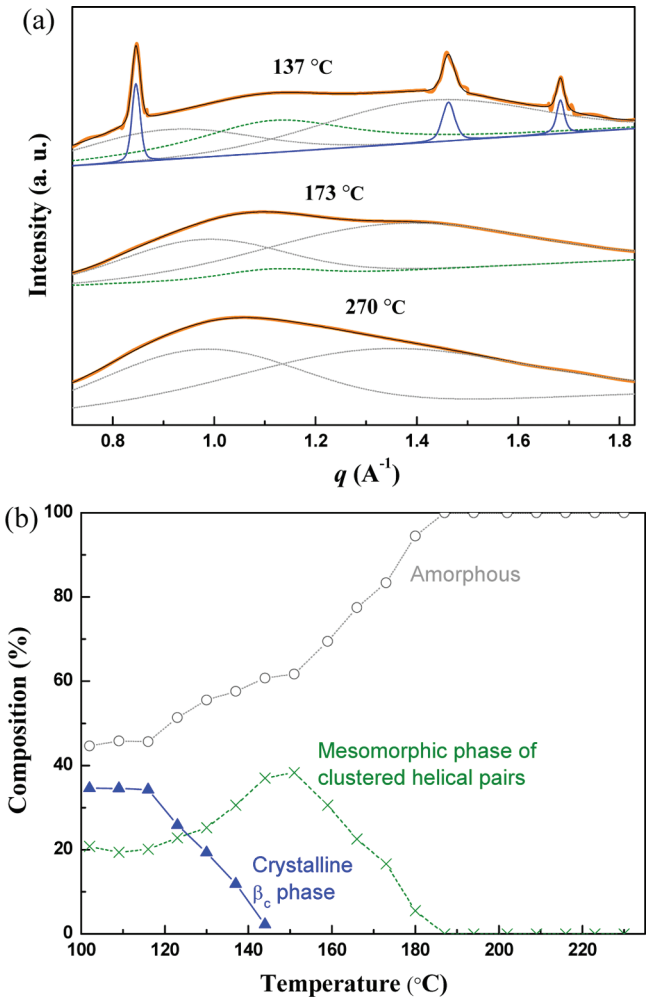

Figure 4. (a) Representative WAXS profiles obtained during cooling (1 °C/min) of racemic PLLA/PDLA blend from 270 °C, fitted with two amorphous peaks (dotted lines), an intermediate halo for clustered helical pairs (dashed lines), and three crystalline peaks (solid thin lines). (b) Corresponding summary of the compositional changes.

mesomorphic phase of intermediate order. The WAXS profile at 270 °C can be decomposed into two broad amorphous peaks which in combination give close description of the amorphous halo centered at scattering vector q ($\equiv 4\pi\lambda^{-1} \sin \theta_B$) $\approx$ 1.1 Å^{-1}. For temperatures below 180 °C (the case of 173 °C is selected for demonstration), a new (i.e., "mesomorphic") component must be incorporated to provide proper description of the halo as continued from higher temperatures. For temperatures below 150 °C (with the case of 137 °C selected for demonstration), crystalline peaks representing (110), (300)/(030), and (220) reflections are further added. The fitted compositions (in terms of fractions of the corresponding peak areas) of amorphous, mesomorphic, and crystalline phases are summarized in Figure 4b. The amorphous fraction (f_a) started to decrease at 180 °C, with the mesomorphic fraction (f_m) increasing up to ca. 0.38 at 150 °C. Upon quick emergence of β_c crystals below 150 °C, f_a continues to decrease albeit at a lower rate, whereas f_m also starts to decrease; both remain significant ($f_a \approx 0.46$ and $f_m \approx 0.20$) at 105 °C where the crystallization process was completed (cf. DSC trace in Figure 3b), leaving a crystalline fraction $f_c \approx 0.34$. This means that nearly half of the pre-existing mesomorphic phase has eventually transformed into β_c crystals, whereas the rest half remains mesomorphic; nearly half of the final crystallinity is contributed by pre-existing mesomorphic phase, whereas the remaining half is contributed by conversion from the amorphous phase.

In view of the already extensive formation of paired helices at 180 °C (cf. Figure 3a), the mesomorphic state is most likely related to clusters of helical pairs, which would be expected to serve subsequently as candidates for primary nucleation of β_c crystals. Figure 5a compares the time-resolved developments of

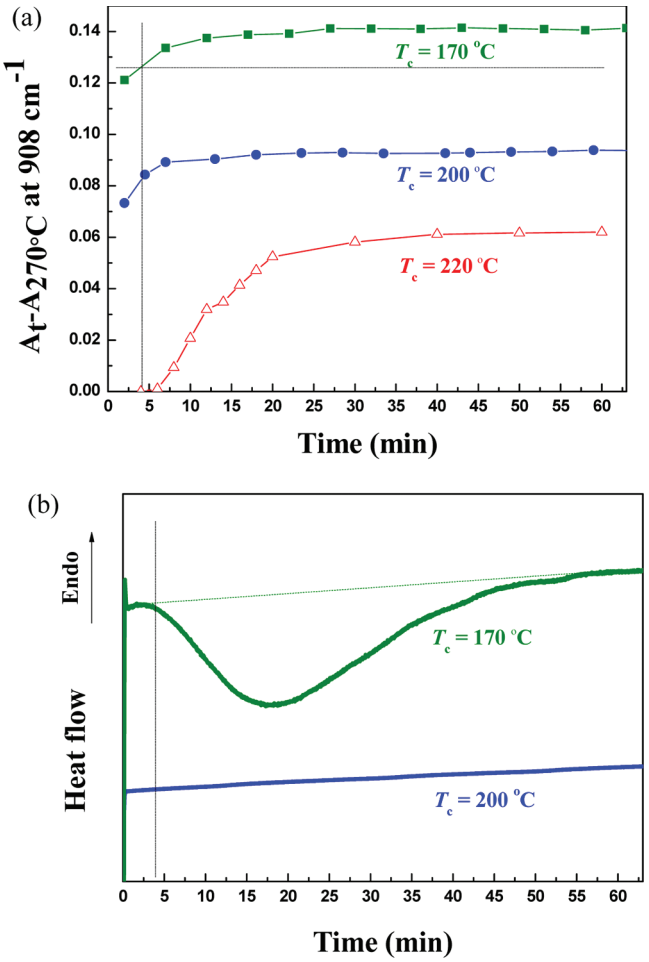

Figure 5. (a) Changes in absorbance of the 908 cm^{-1} band of paired helices as a function of time upon isothermal crystallization at 170, 200, and 220 °C. (b) Corresponding DSC traces, demonstrating progress of crystallization during the period of t_c = 4–55 min at 170 °C in contrast to the complete absence of crystallinity development at 200 °C up to t_c = 63 min.

paired helices in supercooled melt at 170 and 200 °C, whereas Figures 5b and 6 show respectively the corresponding DSC traces and WAXS profiles. It may be observed that isothermal crystallization is well facilitated after a 4 min period of incubation at 170 °C with significant development of paired helices. At a much lower population of paired helices,

dx.doi.org/10.1021/ma2026995 | Macromolecules 2012, 45, 872–878

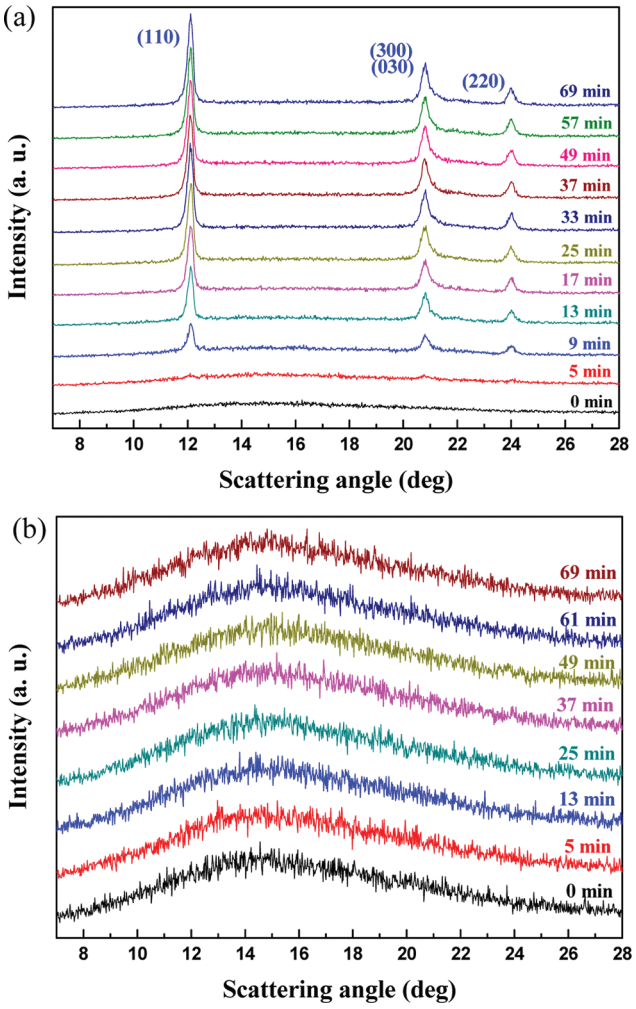

Figure 6. Representative WAXS profiles obtained during isothermal crystallization of the racemic PLLA/PDLA blend at (a) 170 and (b) 200 °C, reaffirming the absence of crystallinity development in the latter case.

isothermal crystallization at 200 °C remains inactivated even after prolonged incubation exceeding 1 h.

Summary of the Phase Transformation Process. To summarize our observations of melt-crystallization in the racemic PLLA/PDLA blend upon slow cooling at 1 °C/min from deeply equilibrated melt at 270 °C, a schematic illustration of the phase transformation process is given in Figure 7. The process begins with the formation of paired $3_2/3_1$ helices. With adequately developed population, clusters of helical pairs are formed, which serve as nucleation sites upon further intracluster ordering. Growth of nuclei into crystals may then proceed.

DISCUSSION

Equilibrated Population of Helical Pairs. Some details in the phase transformation process depicted above deserve further discussion. First, in the absence of crystallization at high temperatures, the formation of paired helices at each temperature is fairly slow, reaching equilibrated population only after ca. 5 min at 200 °C or 20 min at 220 °C (cf. Figure 5a) with an identifiable incubation period of ca. 6 min in the latter case. The presence of an incubation period implies that the pairing process itself involves some fluctuation-induced nucleation-like process at the segmental level, most likely the local adjustment of rotational angles of backbone bonds for matched helical conformation. Nevertheless, as there is no discernible heat of transition, changes in the melt structure are essentially continuous in nature.

On the other hand, the equilibrated population of paired helices is clearly temperature-dependent. Extrapolation of the population (represented by the difference in absorbance) leads to zero population at ca. 260 °C, consistent with the value of equilibrium melting temperature $T_m^\circ = 259 \pm 3$ °C determined via a combination of small-angle X-ray scattering (SAXS), WAXS, and DSC results.[20] The slow formation of such a limited quasi-equilibrium population without going further toward crystallization implies the presence of a balancing force, most likely the elastic force of entangled chains. With decreasing temperature, the energetic preference toward helical pairing is expected to increase while the opposing entropy-driven elasticity decreases, leading to increased population of helical pairs.

Clustering of Paired Helices. The clustering of paired helices is proposed in order to explain the emergence of the broad "mesomorphic" peak in the WAXS profile. This clustering can be a result of (1) induced generation of helical pairs around an existing helical pair or more likely (2) collision/attachment of neighboring pairs through thermally activated fluctuations or Brownian motion. Either of the two routes would be subjected to further balancing force of chain elasticity in the entangled melt. The process should again be continuous, as there is still no identifiable heat of transformation.

Nucleation/Growth of β_c Crystals and Nonvanishing f_m. A more careful examination of Figure 4b reveals that, in the temperature range of 150 to 130 °C, f_a decreased mildly from ca. 0.62 to 0.55; development of the crystalline fraction (up to $f_c \approx 0.20$) was mainly contributed by the decrease in f_m from 0.38

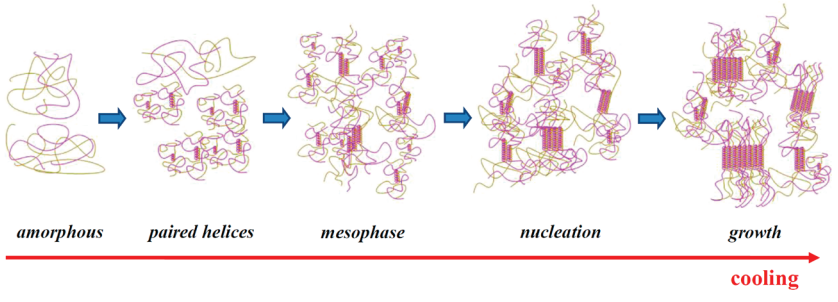

Figure 7. Schematic illustration of the proposed evolution of hierarchical structure during cooling of the racemic PLLA/PDLA blend from equilibrated melt state.

dx.doi.org/10.1021/ma2026995 | Macromolecules 2012, 45, 872–878

to 0.25. This signifies extensive formation of β_c crystals converted from mesomorphic phase and comparatively minor crystal growth in expense of the amorphous fraction. In the subsequent range of 130 to 105 °C, the increase in f_c from 0.20 to 0.34 was mainly contributed by the decrease in f_a (from 0. 55 to 0.46) and a minor decrease in f_m (0.25 to 0.20).

Conversion of clusters of paired helices (i.e., the mesomorphic phase) into primary nuclei of β_c crystals is therefore progressive and incomplete. Mesomorphic clusters are envisioned to fluctuate in size and packing order with the balancing elastic forces or thermal fluctuations, similar to scenarios reported recently on the basis of molecular dynamic simulation for nucleation of polyethylene chains.[21] It may be conceived that only those of highly improved packing order while exceeding the corresponding critical size may activate subsequent growth; this coincides with the classical picture of a discontinuous nucleation process. This critical barrier decreases with decreasing temperature yet remains nonvanishing, leaving significant mesomorphic phase fraction ($f_m \approx 0.20$) along with dominant amorphous fraction ($f_a \approx 0.46$) at the end the crystallization where crystallinity $f_c \approx 0.34$.

On the basis of Figure 4b, crystal growth is envisaged to proceed in two possible ways. Paired helices may be induced at the crystal growth front through surface nucleation (via crystallographic recognition/selection) as described by Hoffman's kinetic theory of crystal growth.[22,23] Nevertheless, to be consistent with the strong decrease of the mesophase fraction in the first half of the crystallization process up to $f_c \approx 0.20$, an alternative route must also be allowed: when an existing mesomorphic cluster of helical pairs is brought into contact with a growing crystal front, the cluster may adsorb onto the growth front and reorient/coalesce with the crystal through layerwise epitaxial reorganization in a manner similar to the coalescence of nanograins during cold crystallization.[24−26] By incorporating key features in both the epitaxial recognition asserted by Lotz[10,27] and the mesomorphic nanoblock attachment advocated by Strobl[28,29] at the crystal growth front, this picture serves to fully explain present observations on the transformation process from amorphous melt to β_c crystals in this particular case of racemic PLLA/PDLA blend.

Incomplete transformation of the mesomorphic phase after the apparent completion of crystallization process below 120 °C may also be taken to imply the presence of further constraints imposed on untransformed precursors. An apparent source of the constraints is the elastic balancing force from stretched chains in the remaining melt phase of highly concentrated entanglements and reduced mobility.[29] The presence of locked-in entanglements in the amorphous phase has been proposed to explain tensile responses and accompanying morphological evolution of semicrystalline polymers.[30]

Suppressed Formation of α Crystals. As a final point, some comments are due on the absence of α crystals of either PLLA or PDLA (cf. Figure 4) in the present study. At a slow cooling rate of 1 °C/min, $3_2/3_1$ helical pairs were extensively developed above 150 °C, resulting in physically cross-linked network of chains which prohibits segregation of PLLA and PDLA chains for development of separate α crystals previously observed[31] to compete with formation of β_c crystals in the temperature range of 150 to 90 °C. This prohibiting effect is certainly absent in the case of cold crystallization of quenched glass of racemic PLLA/PDLA blend; detailed kinetic analysis of this competition between α and β_c phases during cold crystallization is currently ongoing; results will be presented in a separate occasion.

As a final remark, the present FTIR/WAXS evidences correspond mainly to high-resolution molecular processes; hence, we have restrained ourselves from discussing the shape/structure of the mesomorphic clusters of the helical pairs. This latter issue, however, will be addressed with proper analysis of low-resolution SAXS results in the near future.

CONCLUSION

Using FTIR, WAXS, and DSC, we have investigated the structure evolution of PLLA/PDLA stereocomplex during melt crystallization upon slow cooling (1 °C/min) from the equilibrated melt state at 270 °C. On the basis of the characteristic 908 cm^{-1} peak for paired $3_2/3_1$ helices, we show that helical pairs started to emerge in the early stage of cooling below 220 °C. This is followed by the clustering of populated helical pairs into mesomorphic precursors (as indicated by a mesomorphic peak in the WAXS profile) below 190 °C, which subsequently serve as nucleation sites upon further cooling or isothermal standing. The observation that half of the mesomorphic clusters (extensively developed, i.e., $f_m \approx 0.38$, at 150 °C) transformed into crystalline β_c phase is explained by their participation in both the nucleation and the growth of β_c crystals; only half of the final crystalline fraction ($f_c \approx 0.34$ at the end of crystallization process) is attributed to crystal growth via the traditional route of surface nucleation of amorphous chains. We conclude that preformed helical pairs in the melt matrix play a dominant role in the crystallization process of the racemic PLLA/PDLA blend.

ASSOCIATED CONTENT

Supporting Information

Figures S1−S3, showing either difference or second-derivative curves of the FTIR spectra in Figure 1. This material is available free of charge via the Internet at http://pubs.acs.org.

ACKNOWLEDGMENTS

Financial support from the National Science Council (under Grant NSC98 2221 E 007 009 MY3) is gratefully acknowledged. Thanks are also due to Prof. Rong-Ming Ho and Mr. Chien-Wei Huang at NTHU for circular dichroism/polarimetry measurements.

REFERENCES

(1) Bosscher, F.; ten Brinke, G.; Challa, G. *Macromolecules* **1982**, *15*, 1442−1444.
(2) Koennecke, K.; Rehage, G. *Makromol. Chem.* **1983**, *184*, 2679−2691.
(3) Matsubayshi, H.; Chatani, Y.; Tadokoro, H.; Dumas, P.; Spassky, N.; Gigwalt, P. *Macromolecules* **1977**, *10*, 996−1002.
(4) Grenier, D.; Prud'homme, R. E.; Leborgne, A.; Spassky, N. *J. Polym. Sci., Polym. Phys.* **1984**, *22*, 577−587.
(5) Lavallee, C.; Prud'homme, R. E. *Macromolecules* **1989**, *22*, 2438−2446.
(6) Sakakihara, H.; Takakashi, Y.; Tadokoro, H.; Oguni, N.; Tani, H. *Macromolecules* **1973**, *6*, 205−212.
(7) Okihara, T.; Tsuji, M.; Kawaguchi, A.; Katayama, K.; Tsuji, H.; Hyon, H.; Ikada, Y. *J. Macromol. Sci., Macromol. Phys.* **1991**, *B30*, 119−140.
(8) Ikada, Y.; Jamshidi, K.; Tsuji, H.; Hyon, S. H. *Macromolecules* **1987**, *20*, 904−906.
(9) Brizzolara, D.; Cantow, H. J.; Diederichs, K.; Keller, E.; Domb, A. J. *Macromolecules* **1996**, *29*, 191−197.

(10) Cartier, L.; Okihara, T.; Lotz, B. *Macromolecules* **1997**, *30*, 6313−6322.
(11) Zhang, J.; Sato, H.; Tsuji, H.; Noda, I.; Ozaki, Y. *Macromolecules* **2005**, *38*, 1822−1828.
(12) Sarasua, J. R.; Rodriguez, N. L.; Arraiza, A. L.; Meaurio, E. *Macromolecules* **2005**, *38*, 8362−8371.
(13) Kang, S.; Hsu, S. L.; Stidham, H. D.; Smith, P. B.; Leugers, M. A.; Yang, X. *Macromolecules* **2001**, *34*, 4542−4548.
(14) Krikorian, V.; Pochan, D. J. *Macromolecules* **2005**, *38*, 6520−6527.
(15) Zhang, J.; Duan, Y.; Sato, H.; Thuji, H.; Noda, I.; Yan, S.; Ozaki, Y. *Macromolecules* **2005**, *38*, 8012−8021.
(16) Meaurio, E.; Lopez-Rodriguez, N.; Sarasua, J. R. *Macromolecules* **2006**, *39*, 9291−9301.
(17) Pan, P.; Kai, W.; Zhu, B.; Dong, T.; Inoue, Y. *Macromolecules* **2007**, *40*, 6898−6905.
(18) Zhang, J.; Tashiro, K.; Tsuji, H.; Domb, A. J. *Macromolecules* **2007**, *40*, 1049−1054.
(19) Huang, S. J.; Onyari, J. M. *J. Macromol. Sci., Part A: Pure Appl.Chem.* **1996**, *33*, 571−584.
(20) Yang, C. F.; Su, A. C.; Su, C. H.; Jeng, U. Unpublished results.
(21) Lan, Y. K.; Su, A. C. *Macromolecules* **2010**, *43*, 7908−7912.
(22) Hoffman, J. D. *Polymer* **1983**, *24*, 3−26.
(23) Hoffman, J. D.; Miller, R. L. *Polymer* **1997**, *38*, 3151−3212.
(24) Chen, S. H.; Wu, Y. H.; Su, C. H.; Jeng, U.; Hsieh, C. C.; Su, A. C.; Chen, S. A. *Macromolecules* **2007**, *40*, 5353−5359.
(25) Su, C. H.; Jeng, U.; Chen, S. H.; Lin, S. J.; Ou, Y. T.; Chuang, W. T.; Su, A. C. *Macromolecules* **2008**, *41*, 7630−7636.
(26) Su, C. H.; Jeng, U.; Chen, S. H.; Lin, S. J.; Wu, W. R.; Chuang, W. T.; Tsai, J. C.; Su, A. C. *Macromolecules* **2009**, *42*, 6656−6664.
(27) Lotz, B. *Eur. Phys. J. E* **2000**, *3*, 185−194 andreferences cited therein.
(28) Strobl, G. *Eur. Phys. J. E* **2000**, *3*, 165−183 and references cited therein.
(29) Strobl, G. *Rev. Mod. Phys.* **2009**, *81*, 1287−1300.
(30) Men, M.; Rieger, J.; Strobl, G. *Phys. Rev. Lett.* **2003**, *91*, 095502.
(31) Tsuji, H.; Hyon, S. H.; Ikada, Y. *Macromolecules* **1991**, *24*, 5651−5656.